

## The 2010 Pakistan Flood and Russian Heat Wave: Teleconnection of Hydrometeorological Extremes

WILLIAM K. M. LAU

*Earth Science Division, NASA Goddard Space Flight Center, Greenbelt, Maryland*

KYU-MYONG KIM\*

*Goddard Earth Sciences and Technology Center, University of Maryland, Baltimore County, Baltimore, Maryland*

(Manuscript received 3 February 2011, in final form 18 July 2011)

### ABSTRACT

In this paper, preliminary results are presented showing that the two record-setting extreme events during 2010 summer (i.e., the Russian heat wave–wildfires and Pakistan flood) were physically connected. It is found that the Russian heat wave was associated with the development of an extraordinarily strong and prolonged extratropical atmospheric blocking event in association with the excitation of a large-scale atmospheric Rossby wave train spanning western Russia, Kazakhstan, and the northwestern China–Tibetan Plateau region. The southward penetration of upper-level vorticity perturbations in the leading trough of the Rossby wave was instrumental in triggering anomalously heavy rain events over northern Pakistan and vicinity in mid- to late July. Also shown are evidences that the Russian heat wave was amplified by a positive feedback through changes in surface energy fluxes between the atmospheric blocking pattern and an underlying extensive land region with below-normal soil moisture. The Pakistan heavy rain events were amplified and sustained by strong anomalous southeasterly flow along the Himalayan foothills and abundant moisture transport from the Bay of Bengal in connection with the northward propagation of the monsoonal intraseasonal oscillation.

### 1. Introduction

During late July and early August 2010, Pakistan suffered a cluster of torrential rain events, causing the worst flooding in 100 years. According to the reports of the World Meteorological Organization (WMO 2011), 1700 people perished and 1.8 million homes were lost, rendering 20 million people homeless, with an economic loss estimated to be more than \$40 billion (U.S. dollars). At about the same time, western Russia was stricken by a record heat wave and a prolonged drought. Intense and extensive wildfires raged over more than 5000 km<sup>2</sup> of forested area over western Russia. The Russian heat wave and forest fires might have taken over 15 000 lives and cost the economy more than \$15 billion. Both events

represented profound humanitarian disasters that called for detailed scientific investigations. Already a number of studies on the Pakistan flood (Houze et al. 2011; Webster et al. 2011; Wang et al. 2011) and on the Russian heat wave (Schubert et al. 2011; Matsueda 2011; Dole et al. 2011) are now emerging. However, these studies were focused mostly on the details of each individual event separately. In this study, we focus on the teleconnection and feedback mechanisms underlying the Russian heat wave and the Pakistan flood. As such, our paper seeks to provide a new and complementary perspective to the aforementioned studies.

### 2. Data

For this study, we used a combination of in situ, satellite, and reanalysis data to carry out correlative and diagnostic analyses. For rainfall, we used daily gridded rain gauge data from the National Oceanic and Atmospheric Administration's (NOAA) Climate Prediction Center (CPC; Xie et al. 2007) as well as a daily rainfall product (3B42) on a 0.25 × 0.25° latitude–longitude grid from the Tropical Rainfall Measuring Mission (TRMM;

---

\* Current affiliation: GESTAR, Morgan State University, Baltimore, Maryland.

---

*Corresponding author address:* William K. M. Lau, Earth Science Division, NASA Goddard Space Flight Center, Greenbelt, MD 20771.  
E-mail: william.k.lau@nasa.gov

Huffman et al. 2007). Surface temperature was obtained from the Atmospheric Infrared Sounder (AIRS), and fire counts and cloudiness data were from the Moderate Resolution Imaging Spectroradiometer (MODIS) on board the National Aeronautics and Space Administration (NASA) *Aqua* and *Terra* satellites. AIRS is a high-spectral-resolution spectrometer on board the *Aqua* satellite with 2378 bands in the thermal infrared (3.7–15.4  $\mu\text{m}$ ) and 4 bands in the visible (0.4–1.0  $\mu\text{m}$ ). The MODIS fire pixel count has a spatial resolution of  $1 \times 1 \text{ km}^2$  and is determined by a significant increase in radiance at 4  $\mu\text{m}$  relative to 11  $\mu\text{m}$ . It is available from *Terra* and *Aqua* twice daily, night and day. Data and metadata for AIRS and MODIS fire pixel data were available from at the Goddard Earth Sciences Data and Information Service Center (GES DISC; <http://disc.sci.gsfc.nasa.gov/>) and MODIS hotspots/active fires text file FTP site (<http://modis-land.gsfc.nasa.gov/fire.htm>), respectively. For geopotential height, wind, and moisture, we used assimilated data from the NASA Modern Era Retrospective Analysis for Research and Applications (MERRA; Rienecker et al. 2011) available from the Goddard Modeling and Assimilation Office and the GES DISC.

### 3. Background

#### a. Pakistan flood

Located in the northwestern corner of the Indian subcontinent, Pakistan is a relatively dry region. Even during the peak of the monsoon season, July–August, the average total rainfall over the wettest part of the country (northern Pakistan) is of the order of 160–180 mm—a scanty amount compared to a rain total of 1600–2000 mm for the same months over northeastern India and the Bay of Bengal. During July–August 2010, rainfall over northern Pakistan occurred first episodically, with clusters of heavy rain events in 11–12 and 19–22 July (Fig. 1a, bar graph). The most intense heavy rain occurred in 27–29 July, followed immediately by a period of steady moderate-to-heavy rain up to the end of August. Widespread flooding over the Indus River Valley occurred soon after the heavy rain of 27–29 July. We note that while there may be systematic bias in the actual magnitude of the TRMM rainfall over land compared with others, all data show temporal consistency in the occurrence of episodic rain events over northern Pakistan (cf. Webster et al. 2011). Here, we stress that the flooding was unlikely the result of just any singular major heavy rain event, but rather the cumulative effects of all the episodic heavy rain events in July causing increased storm water runoff and saturation of soil moisture, and escalated

further by the steady rain in August. The heavy rain events in July–August plunged approximately one-fifth of the country underwater (Dartmouth Flood Observatory Archives, <http://www.dartmouth.edu/~floods/Current.htm>). As shown in Fig. 1a, the magnitude of the heavy rain events in 2010 far exceeded the  $2\sigma$  deviation based on the 12 years (1998–2009) of TRMM rainfall data. During the 2-week period, 25 July–8 August 2010, CPC rainfall data showed that heavy rain of approximately 500 mm fell in about 10 days in the northern Pakistan Swat Valley—approximately 300% of the climatological rainfall total over the same region in July and August. As evident in the rainfall anomaly pattern shown in Fig. 1b, the heavy rain over northern Pakistan was not isolated geographically, but appeared to be associated with a northeastward shift of the entire South Asian monsoon system, featuring excessive monsoon rainfall over northeastern India along the foothills of the Himalaya, northeastern India and Bangladesh, and northeastern Arabian Sea, coupled to reduced rainfall over central and southern India and the Bay of Bengal.

#### b. Russian heat wave

Summertime atmospheric blocking associated with heat wave, drought, and wildfires occurs commonly over northern Eurasia (Groisman et al. 2007; Girardin et al. 2009). In July–August 2010, a record heat wave developed and prevailed over western Russia. AIRS data show that the surface temperature (upper curve, Fig. 1a) over western Russia rose rapidly around 20 June, remained at a high level for the next 10 days, and intensified from around 18 July, with maximum area-averaged temperature exceeding nearly  $8^{\circ}$ – $10^{\circ}\text{C}$  above the seasonal mean (2003–09). On 18 August, a cold front passed through and brought rain to western Russia, terminating the heat wave. During the two-week period from 25 July to 8 August coinciding with the maximum Pakistan rain, the heat wave expanded to eastern Europe and western Siberia, as shown by the area of positive surface temperature anomaly surrounded by pronounced negative temperature anomalies especially over western Siberia (Fig. 1c). The extreme hot and dry weather spurred ferocious forest fires over the vast taiga regions of western Russia and the Ukraine, as evident in the density of the satellite-observed MODIS fire pixels shown in Fig. 1c. Figure 2 shows the blocking index, as defined by the number of blocked days in the latitude belt  $40^{\circ}$ – $80^{\circ}\text{N}$  during the summer [June–August (JJA)] as a function of longitude. At each longitude, a block is identified when the 5-day mean 500-hPa meridional height gradients exceed given thresholds (Tibaldi and Molteni 1990). Based on this index, the 2010 blocking event was unusual in that 1) its magnitude was more than three times the mean blocking

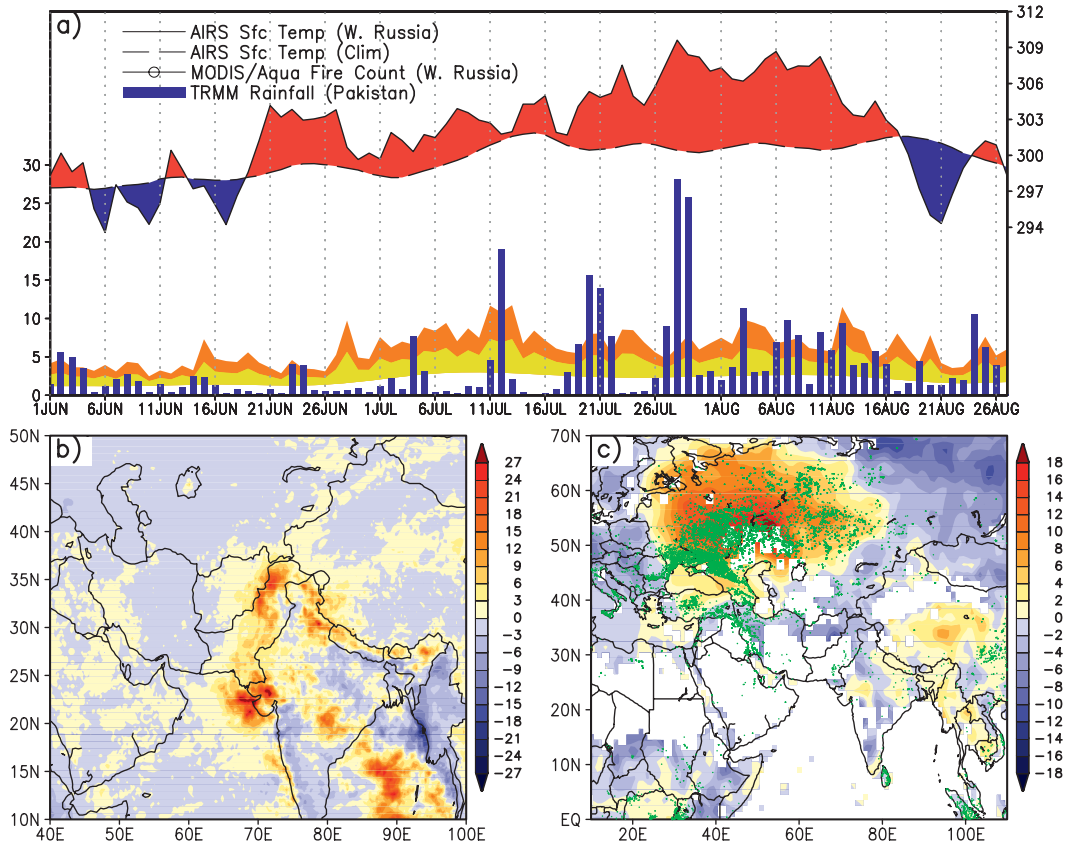


FIG. 1. (a) Time series of AIRS daily surface temperature ( $^{\circ}\text{C}$ ) averaged over western Russia ( $45^{\circ}\text{--}65^{\circ}\text{N}$ ,  $30^{\circ}\text{--}60^{\circ}\text{E}$ ), with positive (negative) deviations from climatology shaded red (blue) and TRMM daily rainfall ( $\text{mm day}^{-1}$ , left ordinate) over northern Pakistan ( $32^{\circ}\text{--}35^{\circ}\text{N}$ ,  $70^{\circ}\text{--}73^{\circ}\text{E}$ ) for 1 Jun–27 Aug 2010. Spatial distribution of (b) TRMM rainfall anomaly over Pakistan and the South Asian monsoon region for the period 25 Jul–8 Aug 2010, (c) AIRS surface temperature anomaly, and MODIS daily fire pixel (green dots) for the same period. The rainfall anomaly ( $\text{mm day}^{-1}$ ) was derived from the base period of 1988–2009, and the surface temperature anomaly ( $^{\circ}\text{C}$ ) from the base period of 2003–09.

index, exceeding by far the  $2\sigma$  level of the climatological variability; 2) it was shifted about  $10^{\circ}$  longitude east of the climatological position near  $25^{\circ}\text{--}30^{\circ}\text{E}$ ; and 3) it covered a longitudinal span  $20^{\circ}\text{--}70^{\circ}\text{E}$ —much larger than the climatology.

#### 4. Teleconnection

To facilitate the discussion of teleconnectivity, evolution, and feedback mechanisms of the Russian heat wave and Pakistan flood, we next describe the quasi-stationary atmospheric patterns during two consecutive 15-day periods, 10–24 July and 25 July–8 August, before and during the transition from the episodic to the steady rain regimes over northern Pakistan, respectively.

##### a. Period I: 10–24 July

This period characterized the development of the Russian heat wave in conjunction with the episodic rainfall

events over northern Pakistan. A 500-hPa blocking high over western Russia was found with a leading trough to its east, spanning western Siberia and regions north of Iran and Pakistan (Fig. 3a). The blocking was associated with a splitting of the 200-hPa jet stream into a northern branch over the polar region ( $60^{\circ}\text{--}70^{\circ}\text{N}$ ,  $10^{\circ}\text{--}60^{\circ}\text{E}$ ) and a more-or-less continuous subtropical branch near  $40^{\circ}\text{N}$  across the domain. As a point for later reference, the 5850-m geopotential height (thick solid line in Fig. 3a), which meandered between  $40^{\circ}$  and  $30^{\circ}\text{N}$ , appeared to separate the extratropics from the tropics. The blocking high and associated wave structure in the midtroposphere, and accompanying circulation moisture fields in the lower troposphere, were very pronounced as shown in the anomaly fields in Figs. 4a,b. At 500 hPa, the blocking high over western Russia was coupled to a bow-shaped deep trough, with two pronounced low-pressure centers (labeled L in Fig. 4a) to its east and another high-pressure feature farther east over central Siberia. The southern

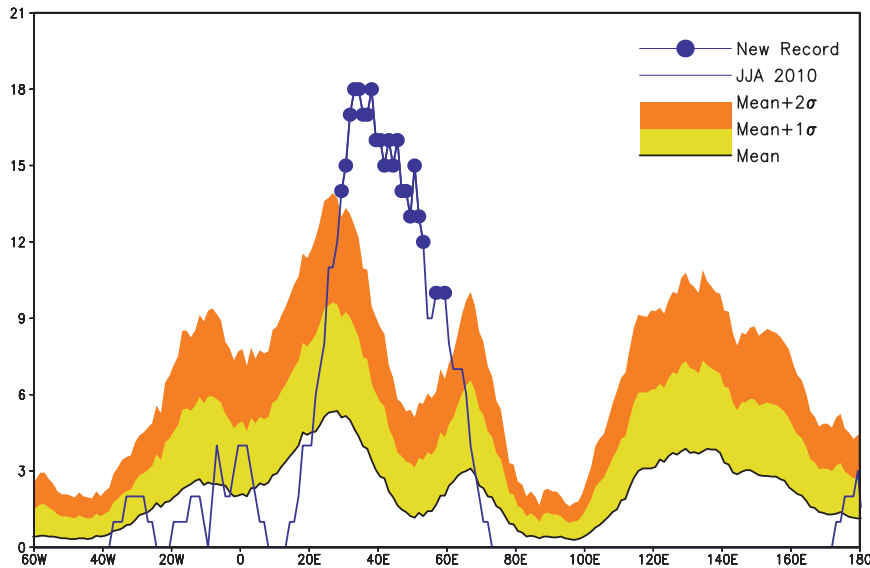


FIG. 2. Number of blocking events at each longitude during boreal summer (JJA) for 2010 (blue) and climatological mean distribution of atmospheric blocking from 1979 to 2009. Yellow and orange layers indicate 1 and 2 std dev from mean, respectively. Blue dots indicate longitudinal locations where the blocks in 2010 were at an all-time high since 1979.

portion of the trough displayed a pronounced southwest-to-northeast tilt, penetrating into the subtropics with a well-defined low center located north of Pakistan. The wave pattern resembled that of a dispersive Rossby wave train (Hoskins and Ambrizzi 1993) emanating from the blocking high over western Russia, and propagating toward the northeast and southeast directions. Matsueda (2011) and Schubert et al. (2011) also noted similar Rossby wave features associated with the 2010 Russian heat wave.

Coupled to the 500-hPa blocking high was a lower-troposphere large-scale anticyclone (Fig. 4b). The equatorward flow on the eastern side of the anticyclone brought widespread cooler and drier (sinking) air over western Siberia to regions farther south, over Kazakhstan and Iran. Over the mountainous region of Afghanistan and Pakistan, the low-level flow was not well organized. However, over the South Asian monsoon region, two distinct branches of anomalous low-level flow could be identified. An anomalous low-level easterly flow from the Bay of Bengal was found over central and northern India, implying an anomalous transport of moisture from the Bay of Bengal to northwestern India. Additionally, an anomalous southerly low-level flow was found over northern Arabian Sea. Analysis (figure omitted) showed that the northern Arabian Sea was warmer than normal in conjunction with the occurrence of La Niña in the tropical Pacific during the summer of 2010. The warmer Arabian Sea could increase evaporation, allowing more moisture transport by the anomalous southerlies into the Gulf of Oman and southern coast of Pakistan (Fig. 4b).

#### b. Period II: 25 July–8 August

During this period, the heat wave intensified and the Russian wildfires grew in area coverage and intensity. At 500 hPa, the quasi-stationary blocking high shifted about  $10^\circ$  eastward in longitude and grew to a very impressive size and magnitude with a characteristic  $\Omega$ -block anticyclonic pattern that split the 200-hPa jet stream into distinct polar and subtropical branches (Fig. 3b). The subtropical branch developed a “kink” west of northern Pakistan with strong jet acceleration downstream of the midtropospheric trough which penetrated from the extratropics to tropics. The pattern of the 5850-m geopotential contour (thick solid line in Fig. 3b) implies strong geostrophic flow associated with the blocking high from near  $60^\circ\text{N}$  to the subtropics below  $30^\circ\text{N}$  (Fig. 3b). The anomaly fields (Fig. 4c) show that the 500-hPa anticyclone shifted eastward over western Russia. The trough at the leading edge of the anticyclone separated distinctly into an extratropical and a tropical component. The tropical component was characterized by a well-defined midtropospheric subtropical low with a closed cyclonic circulation (labeled  $C_1$  in Fig. 4c) near  $25^\circ$ – $35^\circ\text{N}$ , immediately west of northern Pakistan. As discussed previously, the monsoon rain system had shifted northeastward by this time. Indeed,  $C_1$  appeared to be only a part of a large-scale anomalous circulation pattern of the entire South Asian monsoon system, which included the development of a secondary closed cyclonic circulation (marked  $C_2$  in Fig. 4c) over southern Pakistan and northeastern Arabian Sea and an anomalous

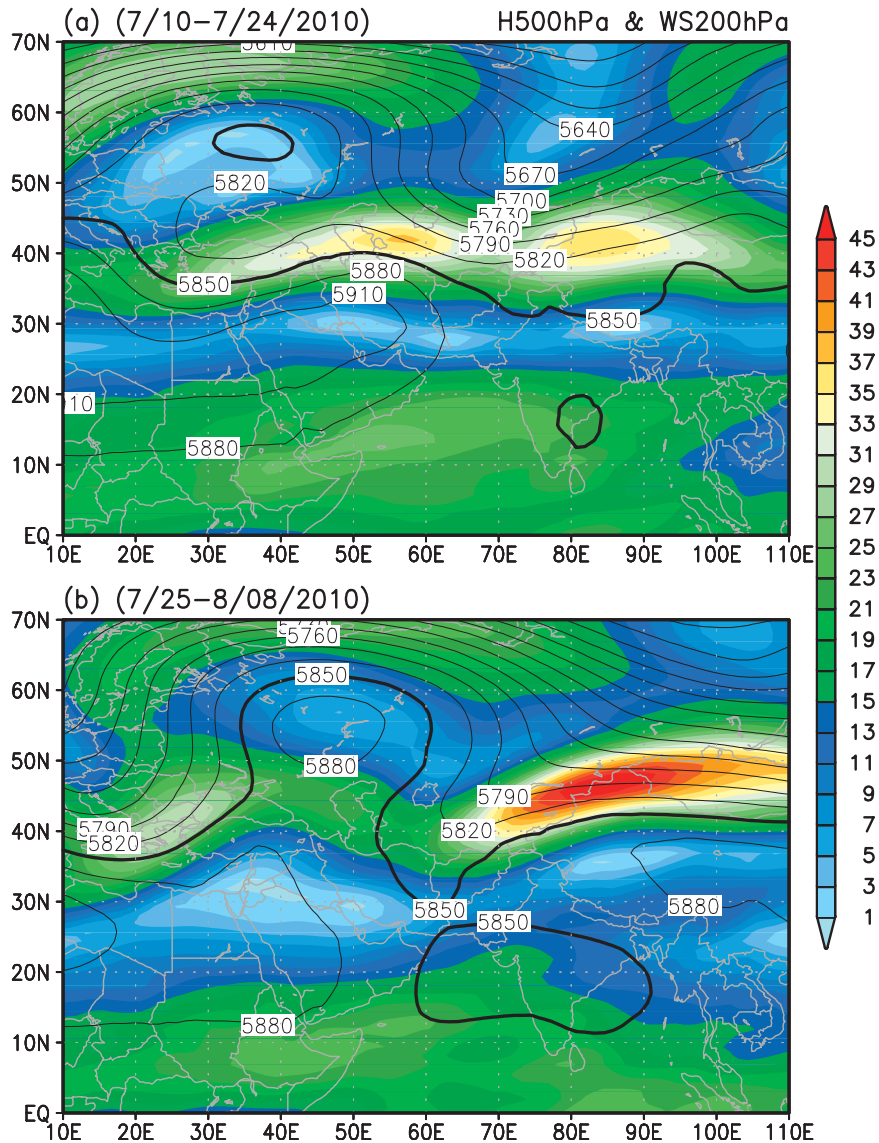


FIG. 3. Spatial patterns of 500-hPa geopotential height (contours) and 200-hPa wind speeds (colors) during periods (a) I and (b) II.

anticyclonic circulation over western China, northeast of the Tibetan Plateau. The tight pressure gradient between the Tibetan high and the cyclonic low system ( $C_1$ – $C_2$ ) forced strong midtropospheric southeasterlies over northern India and southerlies over northern Pakistan, bringing additional moisture from the Bay of Bengal and the northern Arabian Sea. The anomalous midtropospheric low- and high-pressure system over the Tibetan Plateau was also noted by Houze et al. (2011) as a part of the very unusual circulation pattern associated with the 2010 Pakistan flood. The quasi-stationary monsoon cyclonic features were similar to those of hybrid midlatitude and tropical weather systems, called midtropospheric cyclones (MTC), over the subtropical

Asian monsoon region (Mak 1975; Carr 1977; Goswami et al. 1980). The MTCs are well-known rain-bearing systems with a warm core above and cold core below 600 hPa, upper-level divergence, and midtropospheric cyclonic flow and ascent, but generally weak organization near the surface (Krishnamurti and Hawkins 1970).

During period II, in conjunction with the development of the 500-hPa blocking pattern, the low-level anticyclone over northern Europe and Russia also shifted eastward to western Siberia (Fig. 4d). On the southeastern side of the anticyclone, the low-level northeasterly and northerly flow brought a tongue of dry and cold (sinking) air from Siberia to Iran and eastern Pakistan, setting the stage for a confrontation with the warm, moist (rising) air

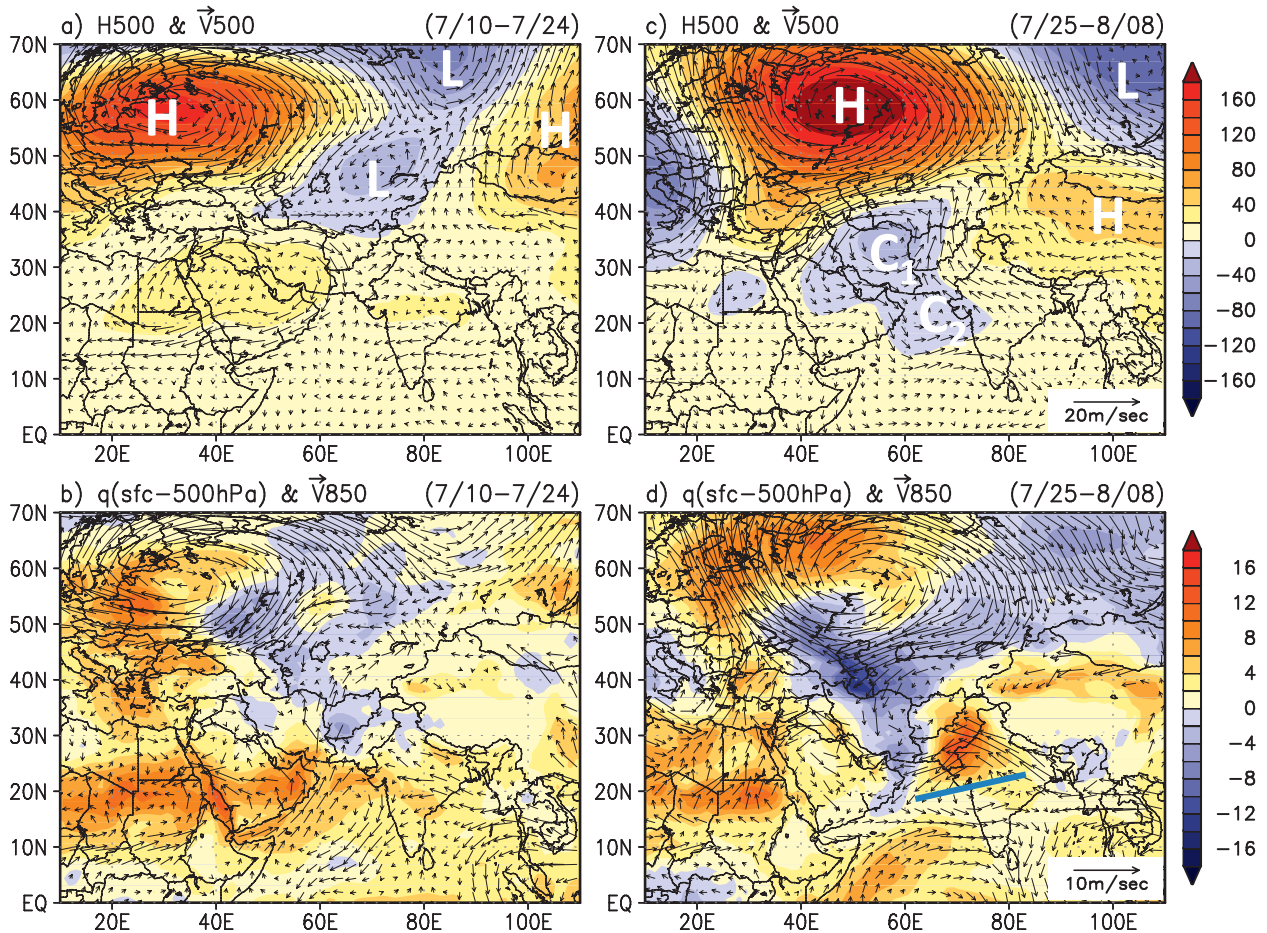


FIG. 4. Spatial patterns of (a) 500-hPa geopotential height (m) and wind anomalies during period I, (b) 850-hPa wind and precipitable water (mm) below 500 hPa during period I, (c) 500-hPa geopotential height and wind anomalies ( $\text{m s}^{-1}$ ) during period II, and (d) anomalous 850-hPa wind and precipitable water during period II. Centers of the blocking high (H) and low (L) and the midtropospheric cyclones ( $C_1$  and  $C_2$ ) are marked. Thick line in Fig. 4d indicates the location of monsoon front. Anomalies were computed based on the climatology of 1979–2009.

transported northwestward from the Bay of Bengal, creating large temperature and moisture contrast favorable for monsoon cyclone development over northern Pakistan. The upper-level disturbances embedded in the leading trough of the Rossby wave were associated with strong upper-level cyclonic vorticity, wind divergence, and 500-hPa ascent (see also Fig. 5) east of the midtropospheric low center. These mid- and upper-tropospheric forcings would act like a pump drawing the low-level southeasterly flow over northern India, along the Indian–Nepal Himalayas, thereby transporting additional moisture from the Bay of Bengal to Pakistan (Fig. 4d). The moist southeasterly flow along the Himalayas foothills was also strengthened by the development of a monsoon trough (thick blue solid line in Fig. 4d) associated with the northward propagation of monsoon intraseasonal oscillations (see further discussion in section 6).

## 5. Triggering and local feedback processes

To illustrate the extratropical triggering of the Pakistan rain events, Fig. 5 shows the 4-day (26–29 July) evolution of 300-hPa relative vorticity, 500 hPa height and vertical velocity, and TRMM rainfall leading up to and during the maximum rain event (27–29 July) over northern Pakistan. The quasi-stationary blocking anticyclone (Fig. 5, left panels) with associated large-scale midtropospheric subsidence (regions shaded blue in Fig. 5, middle panels) over western Russia can be seen in all four days. On 26 July, a day before the occurrence of heavy rain over northern Pakistan, an upper-level V-shaped positive (cyclonic) vorticity filament was formed at the southeastern edge of the 500-hPa anticyclone, dipping into the target region (marked by rectangle in Fig. 5). This vorticity feature moved southward and eastward through the target region in the next three

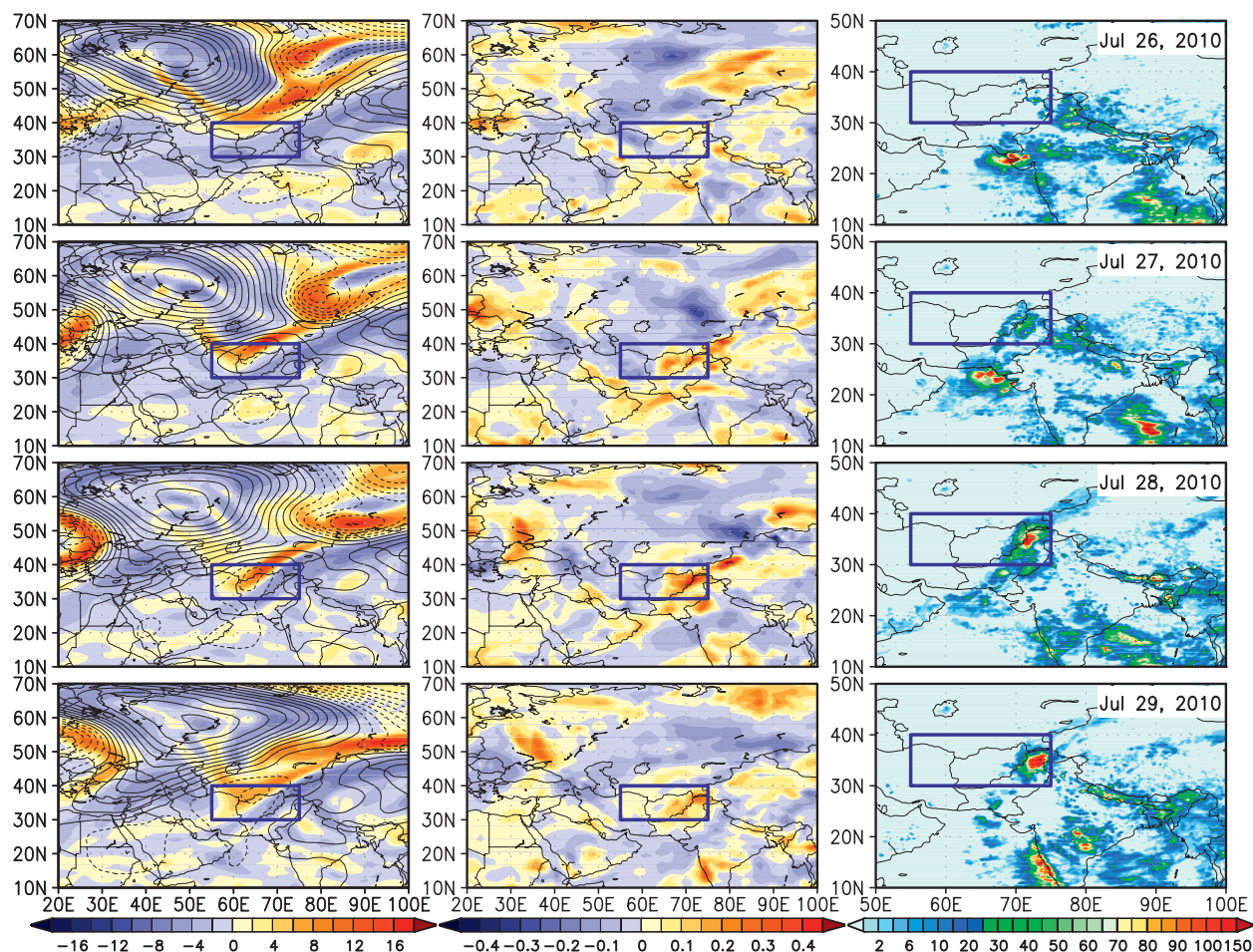


FIG. 5. Daily sequence during 26–29 Jul of MERRA (left) 300-hPa vorticity ( $10^{-5} \text{ s}^{-1}$ ) and 500-hPa height (m) anomalies, (middle) 500-hPa vertical velocity ( $\text{Pa s}^{-1}$ ), and (right) TRMM rainfall (mm). The target region of northern Pakistan and vicinity to the west is indicated by the rectangle. The sign of the vertical velocity (middle) is reversed so that positive value (red) indicates ascending motion.

days (Fig. 5, left panels). It penetrated farthest into the subtropics near  $30^{\circ}$ – $35^{\circ}\text{N}$  during 27–29 July. Strong rising motion was found immediately to the east of the vorticity anomalies (Fig. 5, middle panels), coinciding with the peak rainfall in northern Pakistan (Fig. 5, right panels). Note that on 26 July, the rainfall maximum was still concentrated over the Bay of Bengal, the Himalaya foothills, and northeastern Arabian Sea. By 28–29 July, the maximum rainfall has shifted to over northern Pakistan. Similar sequences of events indicating extratropical triggering were found for the subsequent cluster of heavy rain events centered around 3 and 6 August in period II as well as 12 and 20 July in period I. For more details on the daily variations of surface temperature, upper-tropospheric circulation over Eurasia, and rainfall variations over Pakistan and India for the period 1 July–15 August, an online movie and narrative are available in Lau and Kim (2011).

Next, we present evidence of plausible local feedback mechanisms for the two extreme events and their

connections. For the Russian drought, the positive feedback was likely to occur in association with the below-normal soil moisture indicated by MERRA (not shown) over western Russia at the start of the blocking in early June. As the blocking event commenced around mid-June (see Fig. 1a), the associated subsidence caused adiabatic atmospheric warming and drying by entrainment of dry air from above. The warmer and drier air suppressed rain and clouds and accentuated the initial drying of the land. During period I (Fig. 6a), accompanying the land drying, there was a substantial reduction in cloudiness, up to 20% over the blocking region of western Russia and northeastern Europe (Fig. 6a). The reduced clouds increased downward surface solar radiation with a mean anomaly magnitude of  $\sim 20 \text{ W m}^{-2}$  over the blocking region (Fig. 6b), enhancing surface warming there. The reduced soil moisture led to a reduction in evaporation (approximately  $-10 \text{ W m}^{-2}$ ) latent heat flux from land to atmosphere. The initial drier land, the increased surface

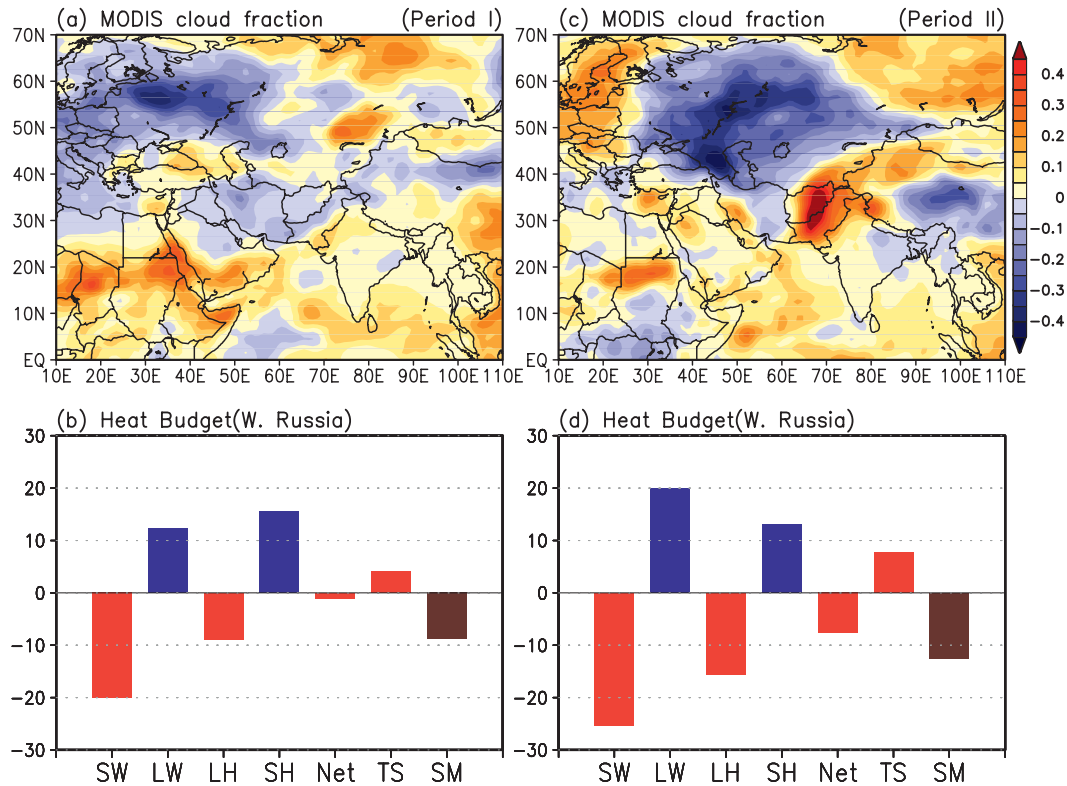


FIG. 6. (top) Distribution of MODIS cloud fraction anomalies for periods (a) I and (c) II. Anomalies were computed based on the climatology of March 2000–February 2010. (bottom) Area mean MERRA shortwave (SW) and longwave (LW) radiation, latent heat (LH) and sensible heat (SH) flux, net flux (Net) at the surface, and soil moisture (SM) averaged over western Russia ( $45^{\circ}$ – $65^{\circ}$ N,  $30^{\circ}$ – $60^{\circ}$ E) for periods (b) I and (d) II. Units are  $W m^{-2}$  for fluxes and fraction ( $\times 100$ ) for soil moisture. Red (blue) color denotes warming (cooling) of the land surface.

shortwave radiation, and the reduced evaporation all conspired to the rapid warming of the surface air and land (see also Fig. 1a). The large increase in sensible heat flux (about  $+15 W m^{-2}$ ) and longwave radiation flux (about  $+10 W m^{-2}$ ) reflected the increasing land surface temperature as the land surface equilibrated energetically. During period II, the surface shortwave continued to increase as more clouds were depleted over even larger areas (Fig. 6c) as the heat wave and the blocking high deepened and shifted westward. The increase in cloudiness associated with heavy rain over northern Pakistan and vicinity is also clearly seen in Fig. 6c. All anomalous surface fluxes remained unchanged in sign compared to period I, but were substantially ( $\sim 25\%$ ) amplified (Fig. 6d). Further reduction in clouds and precipitation (due to lack of surface evaporation) allowed more downward solar radiation, resulting in more warming and desiccation of the land, causing even more reduction in cloud and precipitation and increase in atmospheric stability. Thus the blocking anticyclone was intensified and prolonged, enabling deeper tropical penetration of the upper-level trough and increased transport of cold,

dry Siberian low-level air masses over the Pakistan region. Ferranti and Viterbo (2006) reported similar land surface feedbacks in amplifying the 2003 summertime heat wave over Europe.

Moisture transport integrated between the surface and 850 hPa (Fig. 7a) indicates that during period I, northern Pakistan and the foothill regions were still relatively dry compared to regions to the south. The moist monsoon westerly moisture transport was strongest across the Western Ghat of the Indian subcontinent near  $15^{\circ}$ N. During this period, the Swat Valley region near  $70^{\circ}$ – $75^{\circ}$ E in northern Pakistan developed an above-normal moist environment locally (Fig. 7b), mainly because of moisture transported from the Arabian Sea, increasing the moist instability, and potential convection in the region. However, the synoptic-scale forcing with respect to moisture and temperature was not well organized. The deep layer of anomalous cold air over northern Pakistan would inhibit the development of organized deep convection, while the warmer air to the west appeared to be decoupled from the moisture field. In contrast, during period II, a pronounced tongue of strong northwestward

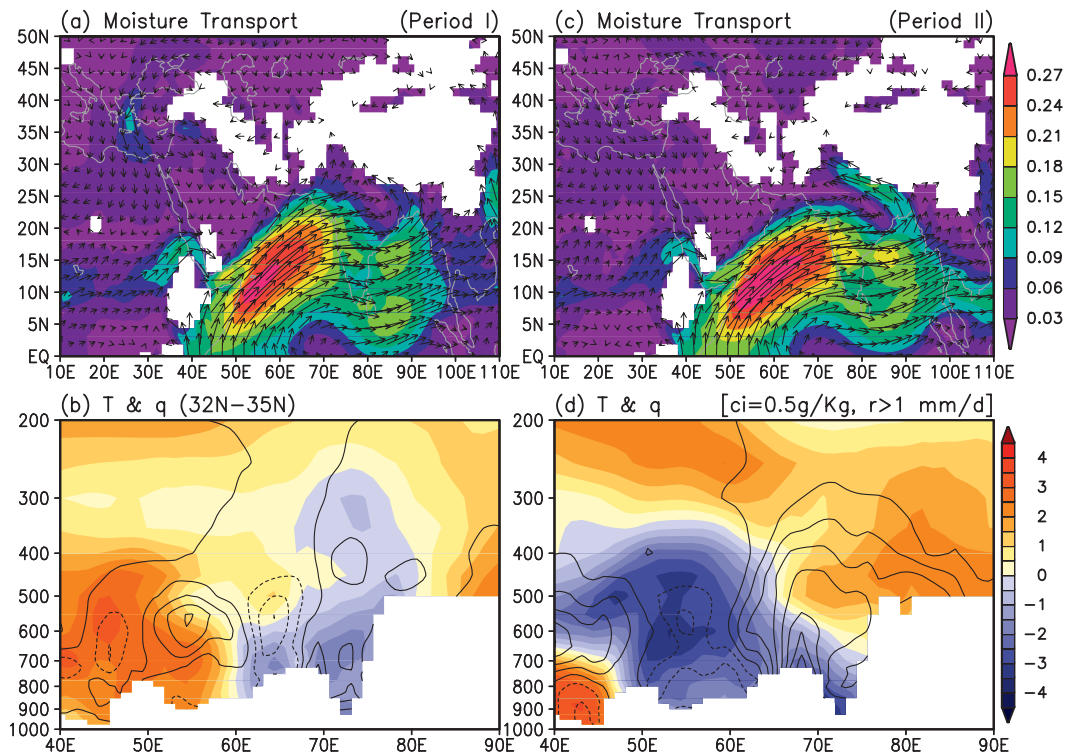


FIG. 7. (top) Distribution of vertically integrated moisture transport between surface to 850 hPa for periods (a) I and (c) II. Amplitude is shown in shading. (bottom) Composite longitude–height cross section of temperature (shading) and moisture (contour) anomalies averaged between 32° and 35°N during rainy days (rain rate > 1 mm day<sup>-1</sup>) in northern Pakistan (see Fig. 1) for periods (b) I and (d) II.

moisture transport brought additional moisture from the Bay of Bengal along the Himalayan foothills to northern Pakistan (Fig. 7c). Here, the synoptic-scale forcing become more organized, with the sinking cold air to the west undercutting and lifting the warm air over northern Pakistan, creating a westward tilt with height (Fig. 7d). The elevated warmer air above 600 hPa over northern Pakistan provided the large-scale structure favorable for the development of warm core MTCs over the Asian monsoon region (Krishnamurti and Hawkins 1970). Over northern Pakistan (65°–70°E), strong ascending motion east of the 500-hPa low was found (see also Fig. 5, middle panels), consistent with the increased moisture supply, as well as frequent occurrence of heavy and steady rain spells over the region during period II. As discussed previously, the source of the low-level cold, dry sinking air was from western Siberia conveyed by the low-level anticyclonic flow from the Russian blocking high, while warm moist air was transported from low-level anomalous southeasterlies from the Bay of Bengal. The warming of the middle and upper troposphere by latent heat release and updrafts from heavy rains of the midtropospheric monsoon cyclones further enhanced low-level moisture from the Bay of Bengal, providing a positive

feedback to the developing monsoon cyclones over the region.

## 6. Role of Monsoon Intraseasonal Oscillation (MISO)

Figure 8a shows the time–latitude cross section of TRMM daily rainfall and the associated monsoon low-level flow across the Pakistan–central India sector (70°–80°E) associated with the MISO during the summer of 2010. The Indian monsoon onset occurred at around 14–15 June as signaled by the sudden appearance of strong steady low-level westerlies and the MISO rainfall reaching 20°N. Subsequently, successive northward surges of MISO rain clusters can be seen reaching the northernmost latitude near the Himalayan foothills (30°–35°N) near the end of July, from whence the rainfall became quite steady until the end of August. At the latitude 30°–35°N, episodic rain events labeled between 1 and 5 can be identified with rainfall maxima shown in Fig. 1a. Events 1–3 were well separated from the main MISO. At the time of occurrence of events 4 (19–20 July) and 5 (27–29 July), there was a strong turning of the low-level winds at 25°–35°N to southeasterlies and easterlies. This was

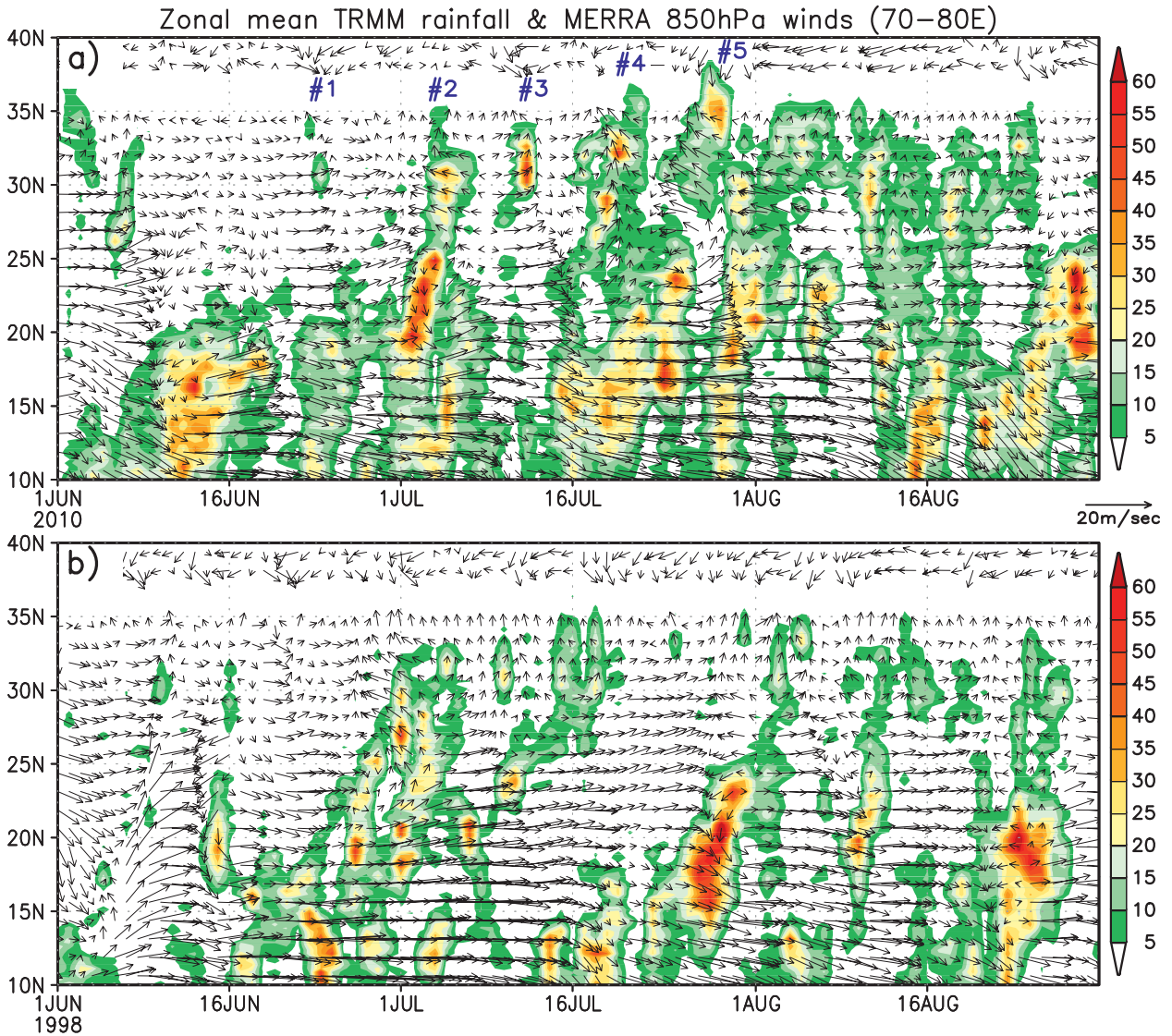


FIG. 8. Latitude–time cross section of TRMM daily rainfall ( $\text{mm day}^{-1}$ ) and MERRA winds at 850 hPa averaged between  $70^\circ$  and  $80^\circ\text{E}$  for (a) 2010 and (b) 1998.

associated with the development of the monsoon trough noted previously in Fig. 4d. From around the end of July to mid-August, the prevailing easterly low-level winds at  $25^\circ$ – $35^\circ\text{N}$  were found at the latitudes of northern Indo-Gangetic Plain and the Himalayan foothills. The easterlies were associated with the westward-moving cyclones along the Himalayan foothills (Houze et al. 2011). It appeared that during the early period of July, while central India and Pakistan were increasingly moistened by the seasonal monsoonal flow, abundant water vapor from the MISO had not yet reached the region. This is in agreement with the recent finding of Wang et al. (2011) that rainfall events over northern Pakistan during July 2010 were episodic, stemming from local instability and

possible triggering by upper-level disturbances. Toward late July and August, as the MISO trough reached northern India and Pakistan, the prevailing low-level southeasterlies transported abundant moisture from the Bay of Bengal to the Himalayan foothills and northern Pakistan. This phase corresponds to the steady monsoon rain discussed earlier. The 2010 Pakistan MISOs were unusual compared to other years in that the associated moisture surges reached far northward and stayed longer in the northern Indian Himalayan foothills region, and that they were associated with strong low-level southeasterlies in northern India and Pakistan ( $30^\circ$ – $35^\circ\text{N}$ ). Examination of other years of TRMM rainfall data indicated that typically, the MISO rainfall and low-level southeasterly wind

signals along the Himalaya foothills were weak or absent. For comparison, the time cross section for summer 1998 (Fig. 8b), which was also a transition year from El Niño to La Niña, shows that, in the latitude belt of northern India and northern Pakistan 30°–35°N, the MISO signals were weak and only episodic rainfall occurred. This suggests that contemporaneous La Niña condition alone may not be sufficient to cause heavy rain events responsible for the 2010 Pakistan flood. Rather, the extreme northward excursion of the MISO may also play a key role. The abnormal conditions associated with the MISOs are also in agreement with Houze et al. (2011), who found that cloud and rain systems normally associated with monsoon depression over the Bay of Bengal were shifted to northern Pakistan during 2010.

At the final revision of this paper, we were brought to the attention of the work by Hong et al. (2011), which showed observational evidence indicating the role of Rossby wave and monsoon surges in triggering the 2010 Pakistan heavy rain, which is consistent with our results. Even though these authors did not address the feedback mechanisms underlying the intensity and prolonged Russian heat wave and the Pakistan heavy rain, their results further strengthen the notion that the two extreme events are physically connected.

## 7. Conclusions

We presented preliminary evidence suggesting that the two extreme events in the summer of 2010 (i.e., the Russia heat wave and the Pakistan flood) were meteorologically connected. Both events were unusual in that the magnitudes of the anomalies far exceeded by more than  $2\sigma$  their respective climatological variability. The Russian heat wave was unusual in size and magnitude and in its eastward location compared to climatology and in the development of a pronounced blocking high with a well-defined  $\Omega$ -flow pattern, a split upper-level jet stream, and deep trough penetrating to the subtropics over northern Pakistan. The Pakistan heavy rain during late July and August was also coincident with the arrival of the northward propagation of the monsoon intraseasonal oscillation, coupled with increased southeasterly moisture transport along the Himalayan foothills from the Bay of Bengal to northern Pakistan.

Based on the above results, we argued that the intense and prolonged atmospheric blocking situation associated with the extreme heat wave over western Russia was instrumental in forcing a large-scale atmospheric Rossby wave train connecting western Russia and the South Asian subtropical monsoon region. Upper-level vorticity perturbations in the leading trough of the Rossby wave train penetrating from the extratropics to the

subtropics triggered upward motion ahead (east) of the perturbations, leading to the development of midtropospheric cyclonic anomalies west of northern Pakistan, with cold core below and warm core above 600 hPa. Our analysis also showed that unusual conditions in the South Asian monsoon region may also play an important role in enhancing the Rossby wave forcing by amplifying and sustaining the Pakistan rainfall events via increased moisture transport from the Bay of Bengal associated with the extreme northward reach of monsoon intraseasonal oscillations over northern India and Pakistan in late July to August 2010. Well-designed numerical experiments are needed to test the proposed hypothesis, and to tease out the relative importance of extratropical versus tropical forcing in leading to the 2010 Pakistan heavy rain events.

*Acknowledgments.* This work was supported by the NASA Interdisciplinary Investigation and the Tropical Rainfall Measuring Mission (TRMM). K.-M. Kim was supported by the Korean Meteorological Administration Research and Development Program under Grant RACS\_2010-2018. We thank two anonymous reviewers for their critical and detailed review of the paper.

## REFERENCES

- Carr, F. H., 1977: Mid-tropospheric cyclones of the summer monsoon. *Pure Appl. Geophys.*, **115**, 1383–1412.
- Dole, R., and Coauthors, 2011: Was there a basis for anticipating the 2010 Russian heat wave? *Geophys. Res. Lett.*, **38**, L06702, doi:10.1029/2010GL046582.
- Ferranti, L., and P. Viterbo, 2006: The European summer of 2003: Sensitivity to soil water initial conditions. *J. Climate*, **19**, 3659–3680.
- Girardin, M. P., A. A. Ali, C. Carcaillet, M. Mudelsee, I. Drobyshev, C. Hely, and Y. Bergeron, 2009: Heterogeneous response of circumboreal wildfire risk to climate change since the early 1900s. *Global Change Biol.*, **15**, 2751–2769, doi:10.1111/j.1365-2486.2009.01869.x.
- Goswami, B. N., R. N. Keshavamurty, and V. Satyan, 1980: Role of barotropic, baroclinic and combined barotropic-baroclinic instability for the growth of monsoon depressions and mid-tropospheric cyclones. *J. Earth Syst. Sci.*, **89**, 79–97.
- Groisman, P. Y., and Coauthors, 2007: Potential forest fire danger over Northern Eurasia: Changes during the 20th century. *Global Planet. Change*, **56**, 371–386.
- Hong, C.-C., H.-H. Hsu, N.-H. Lin, and H. Chiu, 2011: Roles of European blocking and tropical-extratropical interaction in the 2010 Pakistan flooding. *Geophys. Res. Lett.*, **38**, L13806, doi:10.1029/2011GL047583.
- Hoskins, B. J., and T. Ambrizzi, 1993: Rossby wave propagation on a realistic longitudinally varying flow. *J. Atmos. Sci.*, **50**, 1661–1671.
- Houze, J. A., K. L. Rasmussen, S. Medina, S. R. Brodzik, and U. Romatschke, 2011: Anomalous atmospheric events leading to the 2010 floods in Pakistan. *Bull. Amer. Meteor. Soc.*, **92**, 291–298.
- Huffman, G. J., and Coauthors, 2007: The TRMM Multisatellite Precipitation Analysis (TMPA): Quasi-global, multiyear,

- combined-sensor precipitation estimates at fine scales. *J. Hydrometeorol.*, **8**, 38–55.
- Krishnamurti, T. N., and R. S. Hawkins, 1970: Mid-tropospheric cyclones of the southwest monsoon. *J. Appl. Meteor.*, **9**, 442–458.
- Lau, W. K. M., and K. M. Kim, cited 2011: Did the Russian heat wave trigger the Pakistan flood in 2010? [Available online at <http://www.earthzine.org/2011/06/01/did-the-russian-heat-wave-trigger-the-pakistan-heavy-rain-in-2010/>.]
- Mak, M.-K., 1975: The monsoonal mid-tropospheric cyclogenesis. *J. Atmos. Sci.*, **32**, 2246–2253.
- Matsueda, M., 2011: Predictability of Euro-Russian blocking in summer of 2010. *Geophys. Res. Lett.*, **38**, L06801, doi:10.1029/2010GL046557.
- Rienecker, M. M., and Coauthors, 2011: MERRA: NASA's Modern-Era Retrospective Analysis for Research and Applications. *J. Climate*, **24**, 3624–3648.
- Schubert, S., H. Wang, and M. Suarez, 2011: Warm season subseasonal variability and climate extremes in the Northern Hemisphere: The role of stationary Rossby waves. *J. Climate*, **24**, 4773–4792.
- Tibaldi, S., and F. Molteni, 1990: On the operational predictability of blocking. *Tellus*, **42A**, 343–365.
- Wang, S. Y., R. E. Davis, W. R. Huang, and R. R. Gillies, 2011: Pakistan's two-stage monsoon and links with the recent climate change. *J. Geophys. Res.*, **116**, D16114, doi:10.1029/2011JD015760.
- Webster, P. J., V. E. Toma, and H.-M. Kim, 2011: Were the 2010 Pakistan floods predictable? *Geophys. Res. Lett.*, **38**, L04806, doi:10.1029/2010GL046346.
- WMO, 2011: Weather extremes in a changing climate: Hindsight on foresight. WMO-No. 1075, 17 pp.
- Xie, P., M. Chen, S. Yang, A. Yatagai, T. Hayasaka, and Y. Fukushima, 2007: A gauge-based analysis of daily precipitation over East Asia. *J. Hydrometeorol.*, **8**, 607–626.